Supplementary Information for

Lensfree optofluidic plasmonic sensor for real-time and label-free monitoring of molecular binding events over a wide field-of-view

Ahmet F. Coskun[1,3,*], Arif E. Cetin[2,5,*], Betty C. Galarreta[2,4,*], Daniel Adrianzen Alvarez [2], Hatice Altug[2,5,§], and Aydogan Ozcan[1,6,§]

[1] Departments of Electrical Engineering and Bioengineering, University of California, Los Angeles (UCLA), CA 90095, USA
[2] Department of Electrical and Computer Engineering, Boston University, MA 02215, USA
[3] Division of Chemistry and Chemical Engineering, California Institute of Technology, Pasadena, CA, 91125
[4] Pontificia Universidad Catolica del Peru, Departamento de Ciencias-Quimica, Avenida Universitaria 1801, Lima 32, Peru
[5] Bioengineering Department, Ecole Polytechnique Federale de Lausanne (EPFL), Lausanne CH-1015 Switzerland
[6] California NanoSystems Institute, University of California, Los Angeles (UCLA), CA 90095, USA

*These authors contributed equally to this project.

§Correspondence to:
Prof. Aydogan Ozcan, UCLA Electrical Engineering Department, Los Angeles, CA 90095
E-mail: ozcan@ucla.edu
Prof. Hatice Altug, Bioengineering Department, Ecole Polytechnique Federale de Lausanne (EPFL), Lausanne CH-1015 Switzerland
E-mail: hatice.altug@epfl.ch

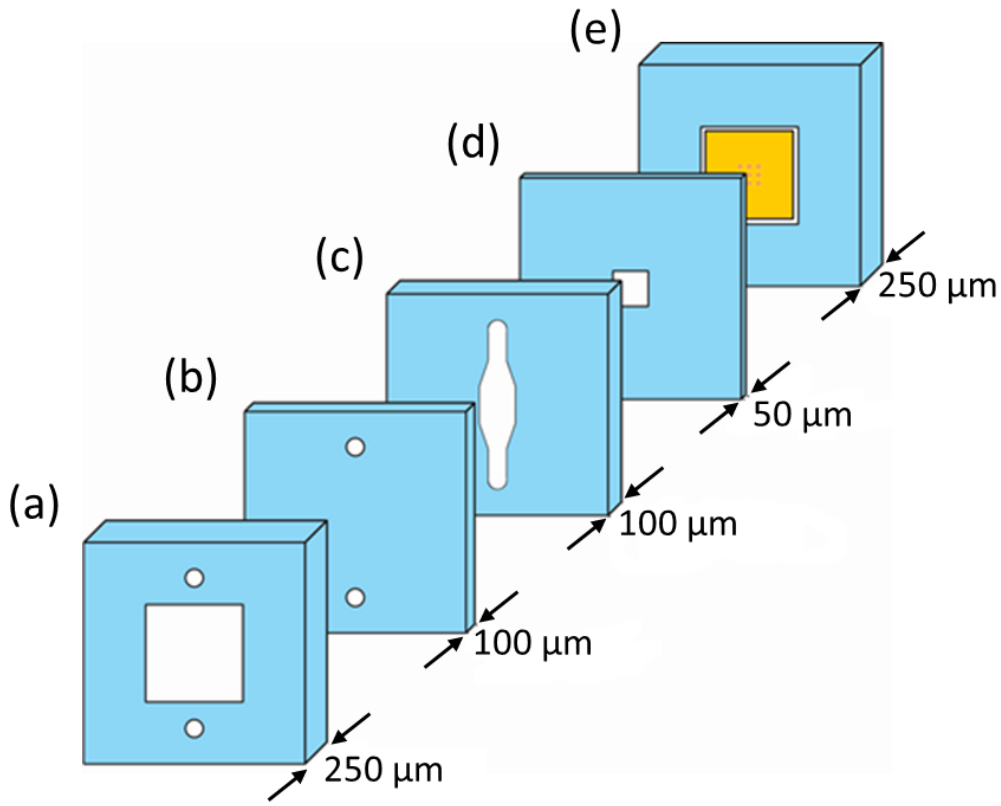

Supplementary Figure 1 Multilayer structure of the disposable microfluidic chamber designed for our handheld plasmonic biosensing device. Four layers of optically clear polyolefin sheet (one side coated with adhesive glue) are assembled with the plasmonic chip. (a-b) Top layers contain the inlet and outlet tube connections. (c) Flow chamber forming the spacer layer. (d) Additional square frame layer, stabilizing the plasmonic chip and minimizing the sensing volume around the plasmonic sensor pixels. (e) Bottom substrate containing the plasmonic nano-hole array.

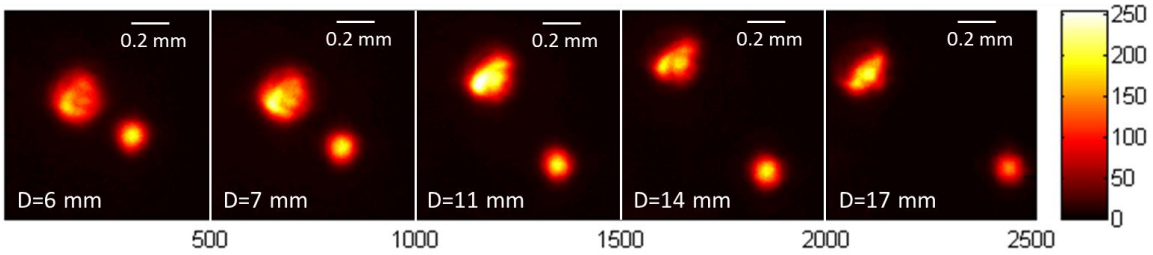

Supplementary Figure 2 Lensfree diffraction patterns generated by our dual-wavelength illumination for different LED separation distances (*D*) ranging from 6 mm to 17 mm.

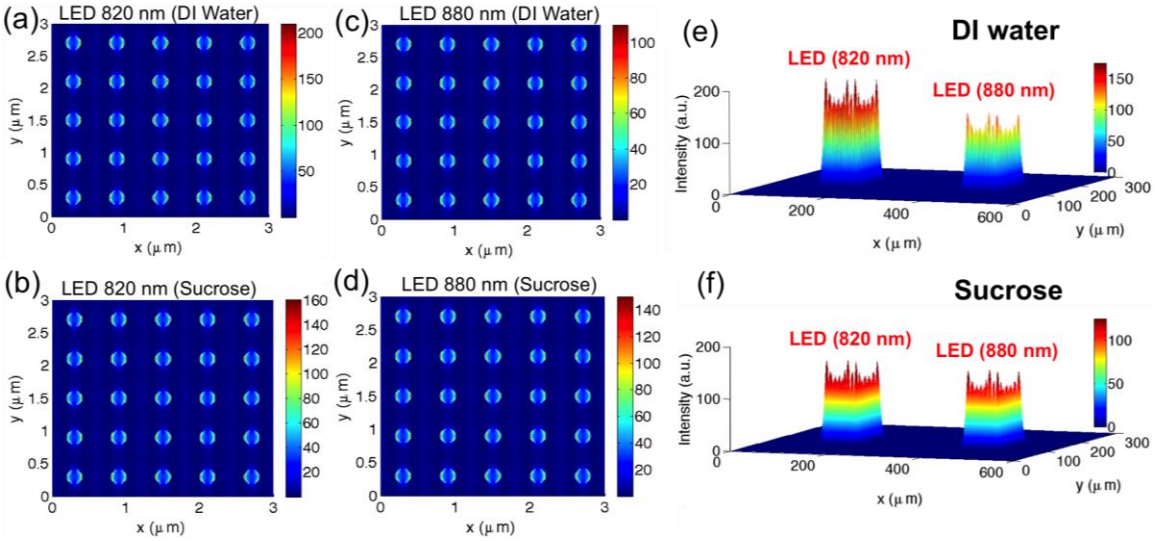

Supplementary Figure 3 Numerical analysis of diffraction patterns. (a-d) Electric-field intensity distributions at $z = 0$ for 5 × 5 nanohole array under two different LED illumination wavelengths (i.e., 820 nm and 880 nm) within two different bulk medium (DI-water and sucrose solution). Note that the nearfield intensities decrease when the nanohole arrays are embedded in a higher refractive index medium (from DI-water to sucrose solution) under 820 nm LED illumination, whereas it increases under 880 nm LED illumination. (e-f) Calculated diffraction patterns at $z = 2\,mm$ for 100 μm × 100 μm microarray pixel containing 28,000 nanohole arrays within two different bulk medium (DI-water and sucrose solution).

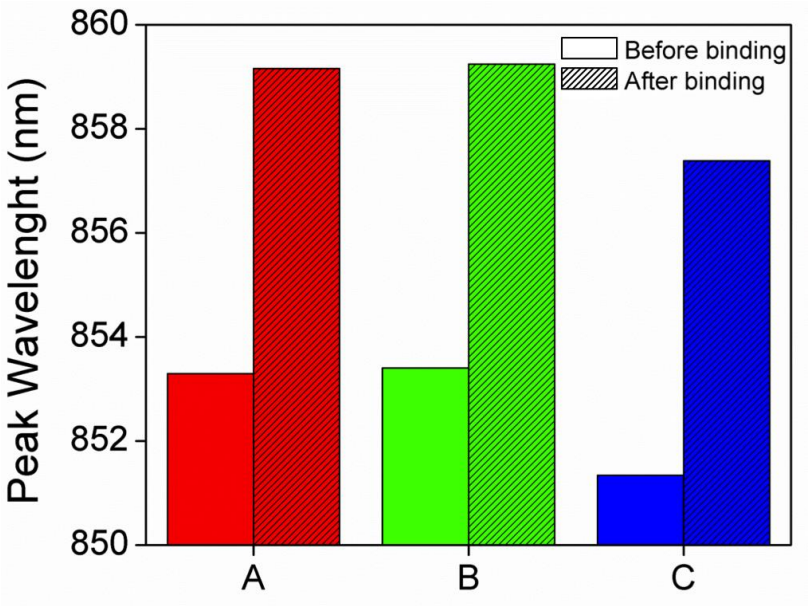

Supplementary Figure 4 For three different plasmonic pixels (A, B, C) located within the same microfluidic chamber, spectral positions of the plasmonic resonance before (t_o) and after (t_f) binding of the protein IgG on the sensing surface covered with protein A/G. Due to the uncontrolled variations in the fabrication of nanostructures, the resonance wavelength may slightly change from one plasmonic pixel to the other one. This difference, however, does not change the shift amount of the peak wavelength upon detection of the same concentration sample.

Theoretical analysis of diffraction patterns

In the presented on-chip biosensing platform, plasmonic interactions occur in the near field of the nano-aperture arrays, which encode the molecular binding events into the transmitted light just after the plasmonic chip. This transmission signal, after propagating 2 mm vertical distance that is due to the separation of the nanoaperture plane and the CMOS active area, is sampled by the CMOS imaging chip, forming "diffraction patterns" in the lensfree images. As described in our previous work[1], these diffraction patterns fall into the Fresnel zone regime, where there is no contribution from evanescent waves. Therefore, we can compute the expected diffraction patterns using a spatial convolution

and Fresnel kernel approach at a given propagation distance based on the following computational flow:

$$\underset{at\ z=\ 0}{Intensity} \rightarrow \begin{bmatrix} Fourier \\ Transform \end{bmatrix} \rightarrow \begin{bmatrix} Fresnel \\ Kernel \end{bmatrix} \rightarrow \begin{bmatrix} Inverse \\ Fourier \\ Transform \end{bmatrix} \rightarrow \underset{CMOS\ at\ z=\ 2\,mm}{\begin{matrix} Intensity \\ Measured\ by \end{matrix}}$$

As an example, for our lensfree imaging geometry, we show the nearfield intensity distribution (at $z = 0$) calculated at the dual LED wavelengths of 820 nm and 880 nm for a 5 × 5 nanohole arrays embedded in DI-water and sucrose solution in Supplementary Figs. 3a-3d. We then compute the expected dual diffraction patterns at $z = 2\,mm$ propagation distance, when simultaneously illuminated by two color LEDs for one plasmonic pixel containing approximately 28,000 nanoholes (100 μm × 100 μm) as shown in Supplementary Figs. 3e-3f.

REFERENCES

1. Cetin, A. E. et al. Handheld high-throughput plasmonic biosensor using computational on-chip imaging. Light Sci. Appl. 3, e122 (2014).